

Smoothed-Hinge Model for Cloth Simulation

Qixin Liang 

the University of Hong Kong & TransGP, Hong Kong

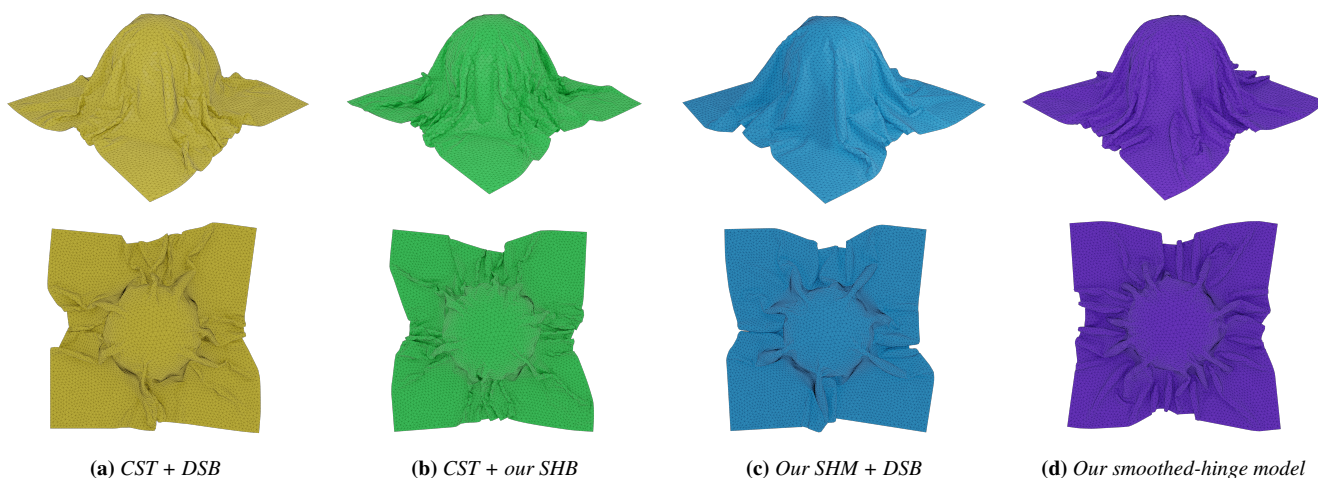


Figure 1: A cotton square cloth (8282 nodes) dropped over a sphere resting on the floor. Sharp creasing artifacts from locking are visible in both (a) the popular discrete shell bending (DSB) model [GHDS03] combined with the constant strain triangle (CST) membrane element and (b) our smoothed-hinge bending (SHB) model combined with CST. The SHB model shows a more complex wrinkle pattern. Sharp creasing artifacts are much reduced when either our smoothed-hinge membrane (SHM) model is blended with (c) the DSB model or (d) SHB model.

Abstract

We present a smoothed-hinge model for cloth simulation, incorporating a smoothed-hinge membrane (SHM) and a smoothed-hinge bending (SHB) component, both found on a triangle-centered elemental patch. SHB derives the directional curvatures across the hinge edges and transforms them into the curvature components used in the continuum shell such that the bending energy can be computed accordingly. Using the corotational method with a small strain/curvature assumption ensures a constant Hessian matrix which enhances the efficiency and stability of implicit solvers. The SHM model, based on a quadratic interpolation scheme, samples membrane strains at the mid-points of hinge edges to address sharp creasing artifacts arising from the locking issue, offering smoother gradients on hinge edges compared to traditional constant strain triangle elements. Incremental potential contact (IPC) manages contact and friction. Our model enriches the family of computational models for realistic cloth simulation, providing a stable and accurate method applicable across diverse clothing scenarios.

CCS Concepts

• **Computing methodologies** → **Physical simulation**;

1. Introduction

The hinge-angle-based bending model combined with constant strain triangle (CST) membrane element exhibits limitations in realistic cloth simulation, such as locking issue [LKJ21] and inconsistent bending behavior [RLR^{*}21]. To address these limitations, we ap-

proximate the membrane and bending deformation fields using interpolated functions constructed from an elemental patch comprising a central triangle and its three adjacent triangles, while retaining the linear triangle mesh structure (see Figure 2). In summary, we contribute a consistent bending model with a constant bending energy Hessian, a membrane model that reduces locking behavior, and

© 2024 The Authors.

Proceedings published by Eurographics - The European Association for Computer Graphics.

This is an open access article under the terms of the Creative Commons Attribution License, which permits use, distribution and reproduction in any medium, provided the original work is properly cited.

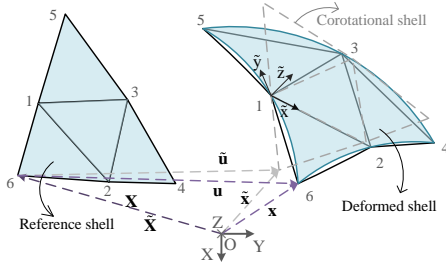


Figure 2: In the reference/deformed configuration, an elemental patch (black line) is fitted to the mid-surface of the thin shell (blue surface). A quantity denoted by a tilde indicates that it is in the corotational configuration.

demonstrate the stability of our model in elastodynamics simulation of fabrics and cloth with large time steps.

2. Thin-Shell Elastic Energy

In this work, we focus on the initial flat thin shell for cloth simulation. The elastic energy of a thin shell can be expressed as:

$$\Psi_{shell} = \frac{1}{2} \int_{\bar{\Omega}} \boldsymbol{\epsilon}_m^T \mathbf{D}_m \boldsymbol{\epsilon}_m d\bar{A} + \frac{1}{2} \int_{\bar{\Omega}} \boldsymbol{\kappa}^T \mathbf{D}_b \boldsymbol{\kappa} d\bar{A}, \quad (1)$$

where $\bar{\Omega}$ represents the reference surface with area element \bar{A} , $\boldsymbol{\epsilon}_m$ is the membrane strain and $\boldsymbol{\kappa}$ is curvature in Voigt notations. In this context, we refer to $\boldsymbol{\kappa}$ as generalized curvature. $\mathbf{D}_m = h\mathbf{E}$ is the membrane stiffness matrix and $\mathbf{D}_b = h^3\mathbf{E}/12$ is the bending stiffness matrix, where h is the shell thickness and the constitutive matrix \mathbf{E} is extracted from the Saint Venant–Kirchhoff model.

3. Geometric Discretization

For a point within a triangle-centered elemental patch in Figure 2, $\mathbf{X} \in R^3$, $\mathbf{u} \in R^3$ and $\mathbf{x} = \mathbf{X} + \mathbf{u}$ represent initial position, displacement and current position, respectively.

Smoothed-hinge membrane model. To compute the strain metric of the central triangle, we employ a one-point integration rule. This approach effectively provides the average value of the strains at the midpoints of the edges:

$$\boldsymbol{\epsilon}_m = \frac{1}{3} \sum_{i=I,II,III} \boldsymbol{\epsilon}_{GL}^i, \quad (2)$$

where $\boldsymbol{\epsilon}_{GL}^i$, $i = I, II, III$ denotes the Green-Lagrangian strain at edge midpoints of the triangle-centered elemental patch.

Smoothed-hinge bending model. The directional curvature vector is

$$\boldsymbol{\kappa}_d = \left\{ \begin{array}{c} \kappa_1 \\ \kappa_2 \\ \kappa_3 \end{array} \right\} = \mathbf{L}_d \mathbf{d}_{\tilde{w}}. \quad (3)$$

Here, \mathbf{L}_d is the directional curvature operator, and $\mathbf{d}_{\tilde{w}}$ aggregates the nodal transverse displacement \tilde{w}_s of an elemental patch. $\boldsymbol{\kappa}$ represents the directional curvature across the hinge edge, under the small strain/curvature assumption, it can be expressed as a linear

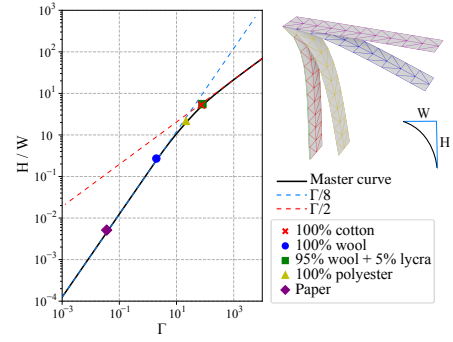


Figure 3: We simulate five strips (30 active nodes) on five real-world materials [LKJ21] and our results agree well with the master curve [RLR*21].

function of nodal transverse displacements [LS09]. Furthermore, the generalized bending curvature of a quadratic fitting surface is

$$\boldsymbol{\kappa} = -(\mathbf{L}_d \mathbf{C}_d)^{-1} \mathbf{L}_d \mathbf{d}_{\tilde{w}}, \quad (4)$$

where \mathbf{C}_d is portrayed as a matrix $\begin{bmatrix} \bar{x}_1^2/2 & \bar{y}_1^2/2 & \bar{x}_1\bar{y}_1/2 \\ \vdots & \vdots & \vdots \\ \bar{x}_6^2/2 & \bar{y}_6^2/2 & \bar{x}_6\bar{y}_6/2 \end{bmatrix}$.

4. Implementation and Results

We use C-IPC [LKJ21] as our foundational simulator, running on a workstation equipped with an Intel Core i9-10980XE CPU (3.00 GHz, 18 cores) and 128 GB of RAM. Qualitative and quantitative results are showcased in Figure 1 and Figure 3.

Acknowledgements

The author is thankful to the anonymous reviewers, the funding support of TransGP and suggestions from Professor K.Y. Sze.

References

- [GHDS03] GRINSPUN E., HIRANI A. N., DESBRUN M., SCHRÖDER P.: Discrete shells. In *Proceedings of the 2003 ACM SIGGRAPH/Eurographics Symposium on Computer Animation* (2003), SCA '03, p. 62–67. URL: <https://dl.acm.org/doi/10.5555/846276.846284>, doi:10.5555/846276.846284.
- [LKJ21] LI M., KAUFMAN D. M., JIANG C.: Codimensional incremental potential contact. *ACM TOG* 40, 4 (Jul 2021), 1–24. URL: <https://doi.org/10.1145/3450626.3459767>, doi:10.1145/3450626.3459767.
- [LS09] LIU X. H., SZE K. Y.: A corotational interpolatory model for fabric drape simulation. *International Journal for Numerical Methods in Engineering* 77, 6 (Feb 2009), 799–823. URL: <https://onlinelibrary.wiley.com/doi/abs/10.1002/nme.2434>, doi:<https://doi.org/10.1002/nme.2434>.
- [RLR*21] ROMERO V., LY M., RASHEED A. H., CHARRONDIÈRE R., LAZARUS A., NEUKIRCH S., BERTAILS-DESCOUBES F.: Physical validation of simulators in computer graphics: a new framework dedicated to slender elastic structures and frictional contact. *ACM TOG* 40, 4 (Jul 2021), 1–19. URL: <https://doi.org/10.1145/3450626.3459931>, doi:10.1145/3450626.3459931.